Nonlinear Dyn (2017) 87:2367–2383
DOI 10.1007/s11071-016-3196-0

ORIGINAL PAPER

Modified adaptive neural dynamic surface control for morphing aircraft with input and output constraints

Zhonghua Wu · Jingchao Lu · Qing Zhou · Jingping Shi

Received: 24 December 2015 / Accepted: 5 November 2016 / Published online: 16 November 2016

Abstract In this paper, a barrier Lyapunov function-based adaptive neural dynamic surface control approach is proposed for morphing aircraft subject to unknown parameters and input–output constraints. Based on the functional decomposition, the longitudinal dynamics can be divided into altitude and velocity subsystems. Minimal learning parameter (MLP) technique-based neural networks are used to estimate the model uncertainties; thus, the amount of online-updated parameters is largely reduced. To overcome the problem of 'explosion of complexity' in the backstepping method, the first-order sliding mode differentiator (FOSD) is introduced to compute the derivative of virtual control laws. Combining MLP and FOSD technique, a composite adaptive neural control scheme is proposed by utilizing an auxiliary system to deal with the input saturation and a barrier Lyapunov function to counteract the output constraints. The highlight is that the proposed neural controller not only owns less online-updated neural parameters, but also has the ability of handling input–output constraints. The stability of the proposed control scheme is established using the Lyapunov theory. Simulation results show that the proposed controller can ensure good tracing performance of the morphing aircraft in the fixed configuration and morphing process.

Keywords Minimal learning parameter · Barrier Lyapunov functions · Input and output constraints · Sliding mode differentiator

Z. Wu (✉) · J. Lu · J. Shi
School of Automation, Northwestern Polytechnical University, Xi'an 710072, China
e-mail: 463897575@qq.com

Q. Zhou
Xi'an Aeronautics Computing Technique Research Institute, AVIC, Xi'an 710068, China

1 Introduction

A growing number of researchers focus on the morphing aircraft field due to its superior flight performance on altering aerodynamic configuration and adapting to different flight environments based on the development of aerotechnology [1]. The wing transition process is complicated and very important for morphing aircraft. During the morphing process, significant variations in mass distribution, aerodynamic forces and moments lead to a complicated time-varying nonlinear dynamical model with internal and external uncertainties [2,3]. Those uncertainties and time-varying characteristics of the morphing aircraft lead to the difficulty in the control system design.

In the existing literatures, most of the control scheme designs of morphing aircraft mainly focus on the longitudinal dynamic model. Based on such model, a pair of linear controllers has been formulated to provide disturbance rejection for a morphing aircraft [4], while the similar idea can also be found in [5]. Subsequently, a finite-time boundness controller is introduced to guarantee the steady flight during the mor-

phing process [6]. In addition, some advanced disturbance rejection control [1] and linear parameter-varying technique [7] have been applied to the control problems of morphing aircraft. However, almost all of the controllers discussed above are built on the basis of linear model and highly depend on the precise prior knowledge of the aerodynamic parameters. Actually, the precise prior knowledge of the aerodynamic parameters is hard to be obtained in the complex atmospheric environment. Nor has morphing aircraft paid the nonlinear dynamics much attention. Therefore, a model-free nonlinear control scheme of morphing aircraft needs to be further investigated. Among numerous control methods including sliding mode control, disturbance observer-based control [8], fractional domain-based technique [9–13] and so on, the approximation-based adaptive back-stepping control scheme via fuzzy logic system (FLS) or neural networks (NN) has received much attention for uncertain nonlinear systems [14,15]. Significant works on adaptive neural/fuzzy control for nonlinear systems with unknown functions are presented in [16–21]. In [16], a self-constructing robust adaptive fuzzy control scheme is proposed for tracking surface vehicles in the presence of uncertainties and disturbances. To overcome the well-known problem of 'explosion of the complexity' in back-stepping method, an improved dynamic surface control (DSC) design has been investigated by introducing first-order low-pass filter or command filter at each step of the adaptive neural back-stepping design procedure [22–28]. Despite the significant progress of the adaptive neural control design for nonlinear systems, studies with input and output constraints on pure-feedback systems are few.

Input saturation caused by the constraints of the magnitude and rate of actuators can degrade the performance of the control system or even lead to instability, if these constraints are neglected in the control design [29]. For dealing with input saturation problem, several auxiliary compensation system-based adaptive control approaches are developed for a class of nonlinear systems [30–32], and those schemes have been also successfully implemented in the flight control [2,33,34]. The effect of input constraints can be properly avoided by introducing an auxiliary design system; unfortunately these schemes cannot be applied to handle the control problem with output constraints which have a significant impact on the system performance. Until now, the design based on barrier Lyapunov function (BLF) to solve nonlinear control problems with output constraints has attracted many scholars' attention [35–46]. The BLF technique has been used to design control methods for output-constrained systems in the strict-feedback form [35–38] and pure-feedback form [39–41]. Moreover, several adaptive neural/fuzzy control schemes are investigated for a multiple-input multiple-output nonlinear system subject to output constraints [42–44]. However, input constraints are not taken into consideration in those control schemes. In [47,48], indirect and direct adaptive fuzzy back-stepping controllers are proposed for uncertain nonlinear systems with input and output constrains. Unfortunately, the control scheme developed in [48] still suffers from the problem of 'explosion of the complexity.' What is more, those schemes only focus on the nonlinear system in strict-feedback form and cannot be directly utilized to the control of morphing aircraft belonging to pure-feedback form. Aforementioned pure-feedback systems in [39–41] have no affine appearance of variables to be used as virtual and actual controllers. Thus, implicit function theorem and the mean value theorem are required to determine each control gain. However, signs and bounds of the derivatives of the nonlinear functions for all the variables are assumed to be known. Therefore, a priori knowledge of the plant dynamics is required to determine these bounds, which may be very difficult to acquire in practical applications [19,21]. Meanwhile, there also exists another restriction in the works [40,41]—too many updated neural parameters are necessary for the control design. To the best of the authors' knowledge, in the existing literatures, this is no result of low computational adaptive neural control for uncertain pure-feedback nonlinear systems with both input and output constraints based on BLF.

This paper investigates a BLF-based adaptive neural DSC approach for the longitudinal dynamics of sweep-back wings morphing aircraft subject to input–output constraints and uncertain parameters. The longitudinal dynamics are decomposed into altitude subsystems and velocity subsystems based on the functional decomposition. In the control design, NNs are employed to approximate unknown nonlinear functions; thus, a priori knowledge of the aerodynamic parameters is no longer required. To overcome the problem of 'explosion of complexity' inherent in the conventional back-stepping method, the first-order sliding mode differentiator (FOSD) is applied to compute the derivatives of virtual control laws. In order to deal with the explosion

of NN' learning parameters, the minimal learning parameter (MLP) technique is used to regulate the norm of NN's weight vector rather than its elements. Consequently, a low computational adaptive neural control scheme is obtained. Meanwhile, filtered signals are applied to avoid the algebraic loop problem encountered in the controller design. Smooth robust compensators are utilized in the virtual and actual controllers to counteract the lumped approximation errors. With the utilization of an auxiliary compensation system and BLF technique, the problems of input saturation and output constraints are eliminated, simultaneously. It is proved that the proposed control scheme can guarantee that all the signals in the closed loop are bounded. Compared with the existed literatures, the main contributions of this paper are shown as follows.

1. Unlike the studies in [35,36,47,48] which only focus on the strict-feedback system with output constraints, this paper further explores the control problem of longitudinal dynamics of morphing aircraft with both input and output constraints, which belongs to a more general class of nonlinear pure-feedback system. Note that, this is also the first application of low computational adaptive neural control of pure-feedback nonlinear systems with input and output constraints in the BLF scope.
2. Different from previous works in [39–41] which need restrictive assumptions and mean value theorem to construct the nonlinear controller, by using Butterworth filter signals, the proposed controller not only avoids the algebraic loop problem in the implementation of the controllers, but also relaxes restrictive assumptions in [39–41].
3. In contrast to the approach in [19,39,40], a barrier Lyapunov technique-based composite adaptive neural method, which is capable of dealing with input–output constraints and the problem of 'explosion of complexity' as well as 'explosion of NN's learning parameters,' is presented and a new type of adaptive laws is constructed by synthesizing the FOSD and MLP in the back-stepping design. This control scheme not only can be used for flight control design, but can also be further extended to the control of a class of nonlinear system in pure-feedback form as [19].

The layout of this paper is as follows. The problem formulation is addressed in Sect. 2. Section 3 describes the control design. Comparative simulation studies are presented in Sect. 4. Conclusions and future works are given in Sect. 5.

2 Problem formulation and preliminaries

2.1 Morphing aircraft model

The control-oriented model of the longitudinal dynamics of a morphing aircraft considered in this study is based on [2]. This model comprises of five state variables (V, h, α, γ, q) and two control inputs (δ_e, T), where V is the velocity, h is the altitude, α is angle of attack, γ is the flight path angle (FPA), q is the pitch rate, δ_e and T denote elevator deflection and thrust force, respectively.

$$\dot{V} = \frac{-D + T\cos\alpha - mg\sin\gamma + F_{Ix}}{m} \tag{1}$$

$$\dot{h} = V\sin\gamma \tag{2}$$

$$\dot{\gamma} = \frac{L + T\sin\alpha - mg\cos\gamma - F_{Ikz}}{mV} \tag{3}$$

$$\dot{\alpha} = -\frac{L + T\sin\alpha - mg\cos\gamma - F_{Iz}}{mV} + q \tag{4}$$

$$\dot{q} = \frac{-\dot{I}_y q - S_x g\cos\theta + M_A + TZ_T + M_{Iy}}{I_y} \tag{5}$$

$$\begin{aligned} F_{Ix} &= S_x\left(\dot{q}\sin\alpha + q^2\cos\alpha\right) \\ &\quad + 2\dot{S}_x q\sin\alpha - \ddot{S}_x\cos\alpha \\ F_{Iz} = F_{Ikz} &= S_x\left(\dot{q}\cos\alpha - q^2\sin\alpha\right) + 2\dot{S}_x q\cos\alpha \\ &\quad + \ddot{S}_x\sin\alpha \\ M_{Iy} &= S_x\left(\dot{V}\sin\alpha + V\dot{\alpha}\cos\alpha - Vq\cos\alpha\right) \end{aligned} \tag{6}$$

where D, L and M_A denote drag force, lift force and pitch moment, respectively. m, I_y and g are the mass of aircraft, moment of inertia about pitch axis and gravity constant. F_{Ix}, F_{Iz}, F_{Ikz} and M_{Iy} represent inertial force and moment caused by morphing process. Z_T is the position of engine in the body axis. S_x denotes the static moment distributed in the body x axis. The related definitions are given as follows:

$$\begin{aligned} &C_D(\zeta) = C_{D0}(\zeta) + C_{D\alpha}(\zeta)\alpha + C_{D\alpha^2}(\zeta)\alpha^2, \\ &\qquad S_x(\zeta) \approx [2m_1 r_{1x} + m_3 r_{3x}], \quad L = C_L(\zeta)QS_w(\zeta), \\ &D = C_D(\zeta)QS_w(\zeta), C_m(\zeta) = C_{m0}(\zeta) + C_{m\alpha}(\zeta)\alpha \\ &\quad + C_{m\delta e}(\zeta)\delta_e + \frac{C_{mq}qc_A(\zeta)}{2V}, \quad Q = \frac{1}{2}\rho_h V^2; \\ &C_L(\zeta) = C_{L0}(\zeta) + C_{L\alpha}(\zeta)\alpha + C_{L\delta e}(\zeta)\delta_e \approx C_{L0}(\zeta) \\ &\quad + C_{L\alpha}(\zeta)\alpha, \quad M_A = C_m(\zeta)QS_w(\zeta)c_A(\zeta) \end{aligned}$$

where ζ is the sweep angle and the other definitions can be found in [2].

2.2 Model transformation

According to [2,33,34], we know that the dynamic model (1)–(5) can be decomposed into altitude subsystem and velocity subsystem since the velocity V is mainly related to T and the altitude h is mainly affected by δ_e.

(a) Altitude subsystem

Define that $x_1 = h$, $x_2 = \gamma$, $x_3 = \theta$, $x_4 = q$ where $\theta = \alpha + \gamma$, $\bar{x} = (x_2, x_3, x_4)$. The altitude subsystem can be converted into the following formulation.

$$\begin{aligned}
\dot{x}_1 &= V x_2 \\
\dot{x}_2 &= f_2(x_2, x_3) + x_3 \\
\dot{x}_3 &= x_4 \\
\dot{x}_4 &= f_4(x_2, x_3, x_4, u) + u \\
y &= x_1, \quad u = -\delta_e
\end{aligned} \tag{7}$$

where y is the output signal of the altitude subsystem (7), $f_2(x_2, x_3)$ and $f_4(x_2, x_3, x_4, u)$ are unknown functions with the formulation $f_2(x_2, x_3) = [L + T\sin(\theta - \gamma) - mg\cos\gamma]/(mV) - \theta$,

$$\begin{aligned}
f_4(x_2, x_3, x_4, u) = &\left[-\dot{I}_y q + (-S_x g\cos\theta\right. \\
&\left. + M_A + TZ_T + M_{Iy})\right]/I_y + \delta_e.
\end{aligned}$$

(b) Velocity subsystem

For the sake of the controller design, velocity subsystem is transformed into the following formulation.

$$\dot{V} = f_V(\bar{x}_V, T) + T \tag{8}$$

where $f_V(\bar{x}_V) = (-D + T\cos\alpha - mg\sin\gamma + F_{Ix})/m - T$ is an unknown nonlinear function.

Remark 1 Since only the cruise phase is considered in this paper, γ is quite small and we can take $\sin\gamma \approx \gamma$ in (2) to simplify the system. In order to transform the altitude system into pure-feedback system, F_{Ikz} in (3) is regarded as an un-modeled term.

2.3 Neural networks

Radial basis function neural networks (RBFNN) are adopted to approximate the continuous function $f(X_{in})$: $R^m \rightarrow R$ which can be expressed as follows [31]:

$$\hat{f}(X_{in}) = \hat{W}^T \Phi(X_{in}) + \varepsilon \tag{9}$$

where X_{in} is the input vector of the NN, $\hat{W}$ is a weight vector of the NN and ε denote the approximation error of the NN. $\Phi(X_{in}) = [\phi_1(X_{in}) \ldots \phi_l(X_{in})]$ is the basis function vector, with $\phi_i(X_{in})$ being Gaussian functions, i.e., $\phi_i(X_{in}) = \exp(-(X_{in} - c_i)^T(X_{in} - c_i)/b_i^2)$ with c_i and b_i denote the centers and widths of the Gaussian functions. The optimal weight value is obtained as

$$W^* = \arg\min_{\hat{W}\in\Omega_f}\left[\sup_{X_{in}\in\Omega_{X_{in}}}\left|\hat{f}(X_{in}|\hat{W}) - f(X_n)\right|\right] \tag{10}$$

where $\Omega_f = \{\hat{W}: ||\hat{W}|| \le \bar{M}\}$ is a valid convex set of the estimated parameter $\hat{W}$. $\bar{M}$ is a design parameter, and Ω_{Xin} is an allowable set of the state vectors. Using the optimal weight value yields

$$f(X_{in}) = W^{*T}\Phi(X_{in}) + \varepsilon^* \tag{11}$$

where ε^* is the optimal approximation error with $|\varepsilon^*| \le \varepsilon_M$.

2.4 Barrier Lyapunov function

In this paper, the following BLF is used [36]

$$\bar{N}_1 = \frac{1}{2}\log\left(\frac{k_b^2}{k_b^2 - z^2}\right) \tag{12}$$

where $\log(\cdot)$ denotes the natural logarithm and k_b is the constraint on z, i.e., $|z| < k_b$. If $|z| = k_b$, the BLF escapes to infinity. It can be shown that $\bar{N}_1$ is positive definite, and C^1 is continuous in the set $|z| < k_b$, and thus, a valid Lyapunov function candidate is in the set $|z| < k_b$.

To process with the design control scheme, the following lemmas are required.

Lemma 1 *The first-order sliding mode differentiator (FSMD) is designed as*

$$\begin{aligned}
\dot{\varsigma}_0 &= -\mu_0|\varsigma_0 - l(t)|^{0.5}\ \ \mathrm{sign}(\varsigma_0 - l(t)) + \varsigma_1 \\
\dot{\varsigma}_1 &= -\mu_1 \mathrm{sign}(\varsigma_1 - \varsigma_0)
\end{aligned} \tag{13}$$

where ς_0 and ς_1 are the states of the system (13), μ_0 and μ_1 are the designed parameters of the first-order

sliding mode differentiator, and $l(t)$ is any known function. $\dot{\varsigma}_0$ can approximate the differential term $\dot{l}(t)$ to an arbitrary accuracy if the initial deviations $\varsigma_0 - l(t_0)$ and $\dot{\varsigma}_0 - \dot{l}(t_0)$ are bounded [49].

Lemma 2 [36] *For any positive constant k_b, the following inequality holds for all z in the interval $|z| < k_b$*

$$\log\left(\frac{k_b^2}{k_b^2 - z^2}\right) < \frac{z^2}{k_b^2 - z^2} \tag{14}$$

Lemma 3 *The following inequality holds for any $w_0 > 0$ and $x \in R$* [27].

$$0 \le |x| - x\tanh\left(\frac{x}{w_0}\right) \le \kappa_0 w_0 \tag{15}$$

where κ_0 is a constant satisfying $\kappa_0 = e^{-(\kappa_0+1)}$, i.e., $\kappa_0 = 0.2785$.

3 Controller design and stability analysis

In this section, adaptive neural DSC and adaptive laws are designed for the altitude and velocity subsystem, respectively. The control scheme is shown in Fig. 1.

Assumption 1 Throughout this work, it is assumed that all of the system states can be measured.

In this paper, $f_2(x_2, x_3)$, $f_4(x_2, x_3, x_4, u)$ and $f_V(\bar{x}_V, T)$ are unknown functions. In order to process the derivation in the following, we define

$$\Delta f_2 = f_2(x_2, x_3) - f_2(x_2, x_{3f}) \tag{16}$$

$$\Delta f_4 = f_4(x_2, x_3, x_4, u) - f_4(x_2, x_3, x_4, u_f) \tag{17}$$

$$\Delta f_V = f_V(\bar{x}_V, T) - f_V(\bar{x}_V, T_f) \tag{18}$$

where x_{3f}, u_f, T_f are the filtered signals defined by [32]

$$x_{3f} = H_L(s)x_3 \approx x_3, \quad u_f = H_L(s)u \approx u, \quad T_f = H_L(s)T \approx T \tag{19}$$

where $H_L(s)$ is a Butterworth low-pass filter. The corresponding parameters of Butterworth filters can be obtained as in [19].

Remark 2 The use of this signal is motivated by [19, 21]. If x_3, u in system (7) and T in system (8) were used as the virtual control, this expression would lead to an algebraic loop and could not be implemented directly. The filtered signals are to avoid the algebraic problem. Meanwhile, it is assumed that the filtered errors Δf_i are bounded.

It is easy to conclude that there exist ideal weight vectors W_2^*, W_4^*, W_V^* such that

$$\begin{cases} f_2(x_2,\ x_{3f}) = W_2^{*T}\Phi_2(x_2,\ x_{3f}) + \varepsilon_2 & |\varepsilon_2| \le \varepsilon_{2M} \\ f_4(x_2,\ x_3,\ x_4,\ u_f) = W_4^{*T}\Phi_4(x_2,\ x_3,\ x_4,\ u_f) + \varepsilon_4 & |\varepsilon_4| \le \varepsilon_{4M} \\ f_V(\bar{x}_V,\ T_f) = W_V^{*T}\Phi_V(\bar{x}_V,\ T_f) + \varepsilon_V & |\varepsilon_V| \le \varepsilon_{VM} \end{cases} \tag{20}$$

where ε_i and ε_{iM} $(i = 2, 4, V)$ denote the approximation errors and their upper bounds, respectively.

Obviously, the ideal weights W_2^*, W_4^*, W_V^* are completely unknown. Therefore, adaptive laws based on Lyapunov function are deduced to update their elements. In order to reduce the computation burden, the MLP technique is employed to estimate the maximum norm of ideal weight vectors; thus, only one parameter needs to be updated online. Those parameters are defined as $\varphi_i = ||W_i^*||^2$ $(i = 2, 4, V)$.

3.1 Velocity controller design

The controller for the velocity subsystem is derived from dynamic inversion method using neural network to approximate the unknown nonlinear function.

Define

$$z_V = V - V_\mathrm{d} - \psi_V \tag{21}$$

where ψ_V is a signal to deal with the saturation effect, and the additional auxiliary system is constructed as follows

$$\dot{\psi}_V = -k_V\psi_V + \Delta T \tag{22}$$

where k_V is a positive design constant, and $\Delta T = T - T_\mathrm{d}$ is the error between the actual control input T and the desired control input T_d.

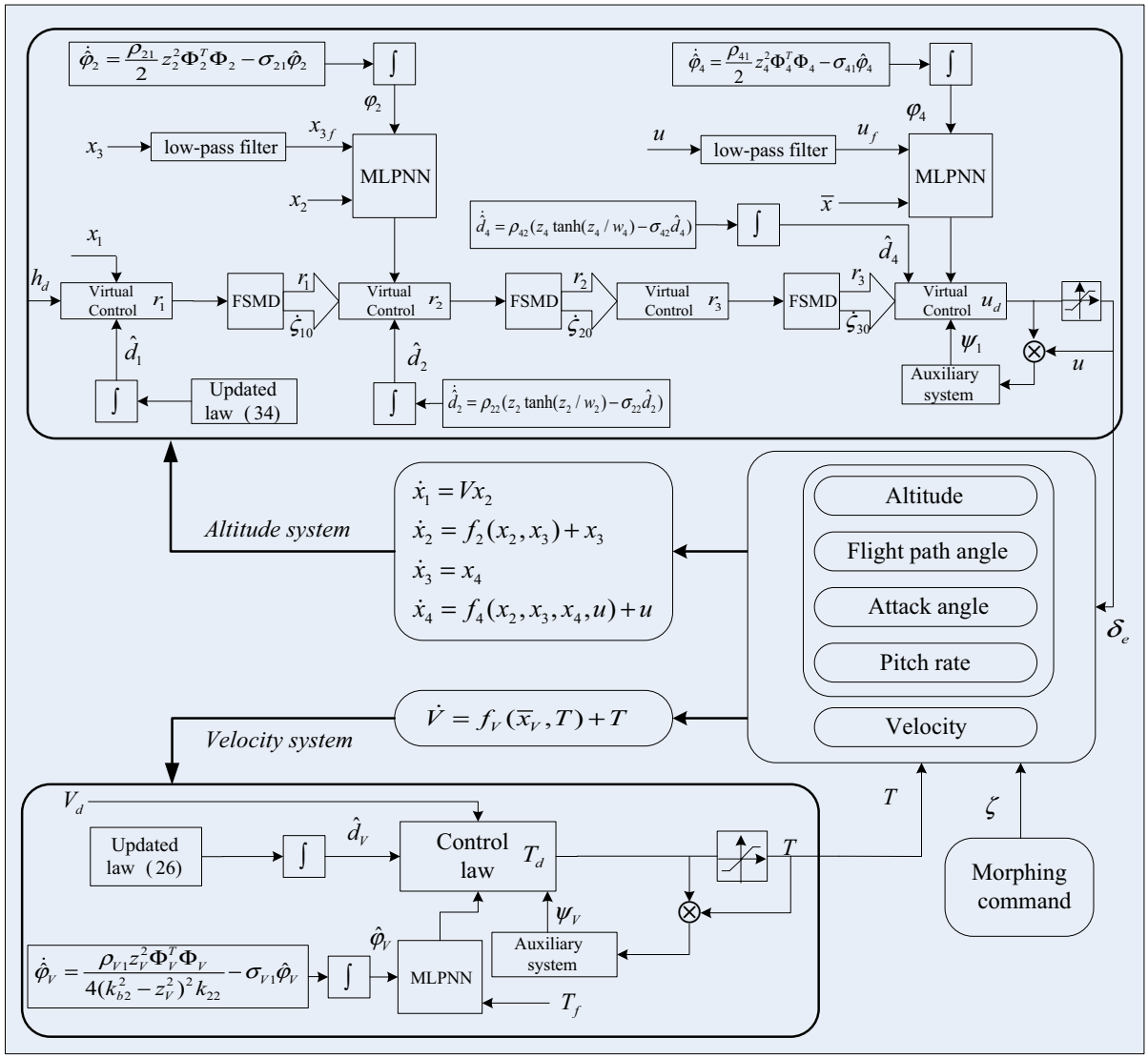

Fig. 1 Control scheme

The time derivative of z_V can be described as

$$\begin{aligned}\dot{z}_V &= \dot{V} - \dot{V}_\mathrm{d} - \dot{\psi}_V = f_V(\bar{x}_V, T) + T - \dot{V}_\mathrm{d} \\ &\quad + k_V\psi_V - \Delta T \\ &= f_V(\bar{x}_V, T_f) + T_\mathrm{d} - \dot{V}_\mathrm{d} + k_V\psi_V + \Delta f_V \\ &= W_V^{*T}\Phi_V(\bar{x}_V, T_f) + T_\mathrm{d} - \dot{V}_\mathrm{d} + k_V\psi_V + d_V\end{aligned} \tag{23}$$

where $d_V = \Delta f_V + \varepsilon_V$, $|d_V| \le d_{VM}$.

On the basis of MLP technique, the desired controller T_d is designed as

$$\begin{aligned}T_\mathrm{d} = &-k_V z_V - \frac{z_V\hat{\varphi}_V\Phi_V^T(\bar{x}_V, T_f)\Phi_V(\bar{x}_V, T_f)}{4(k_{b2}^2 - z_V^2)k_{22}} \\ &- \hat{d}_V \tanh\left[\frac{z_V}{k_{b2}^2 - z_V^2}\frac{1}{w_V}\right] + \dot{V}_\mathrm{d} - k_V\psi_V\end{aligned} \tag{24}$$

where k_V, k_{22} and w_V are positive design parameters. $\hat{d}_V \tanh(z_V/(k_{b2}^2 - z_V^2)/w_V)$ is a robust compensator. $\hat{\varphi}_V$ and $\hat{d}_V$ denote the estimation of φ_V and d_{VM}, respectively.

Consider the following adaptive laws for $\hat{\varphi}_V$ and $\hat{d}_V$,

$$\dot{\hat{\varphi}}_V = \frac{\rho_{V1} z_V^2 \Phi_V^T(\bar{x}_V, T_f)\Phi_V(\bar{x}_V, T_f)}{4(k_{b2}^2 - z_V^2)^2 k_{22}} - \sigma_{V1}\hat{\varphi}_V \tag{25}$$

$$\dot{\hat{d}}_V = \rho_{V2}\left[\frac{z_V}{k_{b2}^2 - z_V^2}\tanh\left(\frac{z_V}{k_{b2}^2 - z_V^2}\frac{1}{w_V}\right) - \sigma_{V2}\hat{d}_V\right] \tag{26}$$

where σ_{V1}, σ_{V2} are positive design parameters.

Invoking (23) and (24) yields

$$\begin{aligned}\dot{z}_V = &-k_V z_V + z_V W_V^{*T}\Phi_V(\bar{x}_V, T_f) \\ &- \frac{z_V\hat{\varphi}_V\Phi_V^T(\bar{x}_V, T_f)\Phi_V(\bar{x}_V, T_f)}{4(k_{b2}^2 - z_V^2)} \\ &+ d_V - \hat{d}_V\tanh\left[\frac{z_V}{k_{b2}^2 - z_V^2}\frac{1}{w_V}\right]\end{aligned} \tag{27}$$

Theorem 1 *Consider the velocity subsystem (8) under assumption 1 and initial condition $|z_V(0)| < k_{b2}$, control law (24), updating laws (25), (26), then the closed-loop signals z_V, $\tilde{\varphi}_V$, $\tilde{d}_V$ are semi-globally bounded. Furthermore, the tracking error z_V and the weights $\tilde{\varphi}_V$, $\tilde{d}_V$ converge to the compact set Ω_{Z_V}, $\Omega_{\tilde{\varphi}_V}$, $\Omega_{\tilde{d}_V}$, respectively, defined by*

$$\begin{cases}\Omega_{Z_V} := \left\{z_V \in R^n, |z_V| \le k_{b2}\sqrt{\left(1 - e^{-2(L_V(0) + C_{V2}/C_{V1})}\right)}\right\} \\ \Omega_{\tilde{\varphi}_V} := \left\{\tilde{\varphi}_V \in R^n, |\tilde{\varphi}_V| \le \sqrt{2\rho_{V1}(L_V(0) + C_{V2}/C_{V1})}\right\} \\ \Omega_{\tilde{d}_V} := \left\{\tilde{d}_V \in R^n, \left|\tilde{d}_V\right| \le \sqrt{2\rho_{V2}(L_V(0) + C_{V2}/C_{V1})}\right\}\end{cases} \tag{28}$$

where C_{V1} and C_{V2} are defined in "Appendix." Meanwhile, the proof of Theorem 1 is also shown in "Appendix."

3.2 Altitude controller design

In order to proceed the design process, the following auxiliary system is constructed to generate ψ_1.

$$\dot{\psi}_1 = \Delta u - k_4\psi_1 \tag{29}$$

where k_4 is a positive design parameter, $\Delta u = u - u_d$, u is the actual control input to the system and u_d is the control input to be designed. The relationship of u_d and u can be expressed as follows:

$$u = \text{sat}(u_d) = \begin{cases}\text{sign}(u_d)u_d^+, & \text{if } |u_d| > u_d^+ \\ u_d, & \text{else}\end{cases} \tag{30}$$

where u_d^+ is a positive constant that quantizes the bound of input saturation.

The following coordinate change is constructed to facilitate the control design:

$$\begin{cases}z_1 = x_1 - y_d \\ z_2 = x_2 - r_1 \\ z_3 = x_3 - r_2 \\ z_4 = x_4 - r_3 - \psi_1\end{cases} \tag{31}$$

where r_1, r_2 and r_3 are the virtual controllers to be designed at step 1, 2 and 3, respectively. $y_d = h_d$ is the reference signal.

The control scheme for the altitude subsystem is developed in the framework of back-stepping technique, which contains four-step recursive design procedure.

Step 1 The time derivative of $z_1 = x_1 - y_d$ is expressed as

$$\dot{z}_1 = \dot{x}_1 - \dot{y}_d = Vx_2 - \dot{y}_d = V(z_2 + r_1) - \dot{y}_d \tag{32}$$

The virtual controller r_1 is designed as

$$r_1 = -k_1 z_1 - \frac{z_1}{2(k_{b1}^2 - z_1^2)} + \frac{\dot{y}_d}{V} - z_1\hat{d}_1\tanh\left(\frac{z_1^2}{k_{b1}^2 - z_1^2}\frac{1}{w_1}\right) \tag{33}$$

where k_1 and w_1 are positive parameters; $\hat{d}_1 z_1 \tanh(z_1^2/(k_{b1}^2 - z_1^2)/w_1)$ is a robust compensator; $\hat{d}_1$ denotes the estimation of d_{1M}. $d_1 = -\dot{V}/(2V^2)$ is the lump error with upper bound d_{1M}, that is $|d_1| \le d_{1M}$.

Now we consider the adaptive law given as follows

$$\dot{\hat{d}}_1 = \rho_{12}\left[\frac{z_1^2}{k_{b1}^2 - z_1^2}\tanh\left(\frac{z_1^2}{k_{b1}^2 - z_1^2}\frac{1}{w_1}\right) - \sigma_{12}\hat{d}_1\right] \tag{34}$$

where ρ_{12} and σ_{12} are positive design parameters.

Invoking (32) and (33), one has

$$\dot{z}_1 = V\left(z_2 - k_1 z_1 - \frac{z_1}{2(k_{b1}^2 - z_1^2)} - z_1\hat{d}_1\tanh\left(\frac{z_1^2}{k_{b1}^2 - z_1^2}\frac{1}{w_1}\right)\right) \tag{35}$$

In order to avoid the tedious analytical computations involved in the control law of step 2, using Lemma 1, the following first-order sliding mode differentiator is adopted to estimate $\dot{r}_1$.

$$\dot{\varsigma}_{10} = -\mu_{10}|\varsigma_{10} - r_1|^{0.5}\text{sign}(\varsigma_{10} - r_1) + \varsigma_{11}$$
$$\dot{\varsigma}_{11} = -\mu_{11}\text{sign}\,(\varsigma_{11} - \varsigma_{10}) \tag{36}$$

where ς_{10}, ς_{11} are the states of the system (36), and μ_{10}, μ_{11} are the positive design constants.

According to (36) and Lemma 1, we have

$$\dot{r}_1 = \dot{\varsigma}_{10} + \tau_1 \tag{37}$$

where τ_1 is the estimation error with $|\tau_1| \leq \bar{\tau}_1$.

Step 2 The differentiation of z_2 is obtained as follows:

$$\begin{aligned}\dot{z}_2 &= \dot{x}_2 - \dot{r}_1 = f_2(x_2, x_3) + x_3 - \dot{r}_1 \\ &= z_3 + r_2 - \dot{r}_1 + f_2(x_2, x_3) - f_2(x_2, x_{3f}) \\ &\quad + W_2^{*T}\Phi_2(x_2, x_{3f}) + \varepsilon_2 \\ &= z_3 + r_2 - \dot{r}_1 + W_2^{*T}\Phi_2(x_2, x_{3f}) + d_2 \end{aligned} \tag{38}$$

where $d_2 = \Delta f_2 + \varepsilon_2$. d_2 is bounded, and there exists an unknown constant $d_{2M} > 0$ such that $|d_2| \leq d_{2M}$.

Based on MLP technique, the virtual controller r_2 is designed as

$$\begin{aligned} r_2 = &-k_2 z_2 - \frac{1}{2}\hat{\varphi}_2 z_2 \Phi_2^T(x_2, x_{3f})\Phi_2(x_2, x_{3f}) + \dot{\varsigma}_{10} \\ &-\hat{d}_2 \tanh\left(\frac{z_2}{w_2}\right) \end{aligned} \tag{39}$$

where k_2 and w_2 are positive design parameters. $\hat{d}_2 \tanh(z_2/w_2)$ is a robust compensator. $\hat{\varphi}_2$ and $\hat{d}_2$ denote the estimations of φ_2 and d_{2M}, respectively.

The structure of adaptive control laws is expressed as follows

$$\dot{\hat{\varphi}}_2 = \frac{\rho_{21}}{2} z_2^2 \Phi_2^T(x_2, x_{3f})\Phi_2(x_2, x_{3f}) - \sigma_{21}\hat{\varphi}_2 \tag{40}$$

$$\dot{\hat{d}}_2 = \rho_{22}\left[z_2 \tanh\left(\frac{z_2}{w_2}\right) - \sigma_{22}\hat{d}_2\right] \tag{41}$$

Substituting (39) into (38), (38) can be rewritten as

$$\begin{aligned}\dot{z}_2 = &\, z_3 - k_2 z_2 + W_2^{*T}\Phi_2(x_2, x_{3f}) \\ &- \frac{1}{2}\hat{\varphi}_2 z_2 \Phi_2^T(x_2, x_{3f})\Phi_2(x_2, x_{3f}) \\ &+ d_2 - \hat{d}_2 \tanh\left(\frac{z_2}{w_2}\right) + \dot{\varsigma}_{10} - \dot{r}_1 \end{aligned} \tag{42}$$

The following first-order sliding mode differentiator is adopted to estimate $\dot{r}_2$.

$$\dot{\varsigma}_{20} = -\mu_{20}|\varsigma_{20} - r_2|^{0.5}\text{sign}(\varsigma_{20} - r_2) + \varsigma_{21}$$
$$\dot{\varsigma}_{21} = -\mu_{21}\text{sign}(\varsigma_{21} - \varsigma_{20}) \tag{43}$$

where ς_{20}, ς_{21} are the states of the system (36), and μ_{20}, μ_{21} are positive design constants.

From (43) and Lemma 1, we have

$$\dot{r}_2 = \dot{\varsigma}_{20} + \tau_2 \tag{44}$$

where τ_2 is the estimation error with $|\tau_2| \leq \bar{\tau}_2$.

Step 3 The differentiation of z_3 is obtained as follows:

$$\dot{z}_3 = \dot{x}_3 - \dot{r}_2 = (x_4 - r_3) + r_3 - \dot{r}_2 = z_4 + r_3 - \dot{r}_2 + \Psi_1 \tag{45}$$

The virtual control law r_3 is designed as

$$r_3 = -k_3 z_3 + \dot{\varsigma}_{20} - \psi_1 - z_2 \tag{46}$$

where $k_3 > 0$ is a design constant. ψ_1 is an auxiliary compensation signal.

Substituting (46) into (45) yields

$$\dot{z}_3 = z_4 - z_2 - k_3 z_3 + \dot{\varsigma}_{20} - \dot{r}_2 = z_4 - z_2 - k_3 z_3 - \tau_2 \tag{47}$$

Consider the following inequality

$$-\tau_2 z_3 \leq \frac{1}{2k_{11}} z_3^2 + \frac{k_{11}}{2}\bar{\tau}_2^2 \tag{48}$$

where $k_{11} > 0$. Note that the constants k_{11} in (48) is not used in the implementation of the control law, but rather, it is only used to analytically show the stability of the control system. Therefore, the constant k_{11} is only required to exist, but may remain unknown. Moreover, it does not need to be estimated in the implement of the controller.

As done previously, the following first-order sliding mode differentiator is employed to estimate $\dot{r}_3$:

$$\dot{\varsigma}_{30} = -\mu_{30}|\varsigma_{30} - r_3|^{0.5}\text{sign}(\varsigma_{30} - r_3) + \varsigma_{31}$$
$$\dot{\varsigma}_{31} = -\mu_{31}\text{sign}(\varsigma_{31} - \varsigma_{30}) \tag{49}$$

where ς_{30}, ς_{31} are the states of the system, and μ_{30}, μ_{31} are the positive design constants.

Thus, we have

$$\dot{r}_3 = \dot{\varsigma}_{30} + \tau_3 \tag{50}$$

where τ_3 is an estimation error with $|\tau_3| \leq \bar{\tau}_3$.

Step 4 In this step, the actual controller u will be developed. The differentiation of z_4 can be obtained as follows:

$$\begin{aligned}\dot{z}_4 &= f_4(x_2, x_3, x_4, u) + u - \dot{r}_3 - \Delta u + k_4\psi_1 \\ &= f_4(\bar{x}, u_f) + u_{\mathrm{d}} - \dot{r}_3 + k_4\psi_1 + \Delta f_4 \\ &= W_4^{*T}\Phi(\bar{x}, u_f) + u_{\mathrm{d}} - \dot{r}_3 + k_4\psi_1 + d_4 \end{aligned} \tag{51}$$

where $d_4 = \Delta f_4 + \varepsilon_4$ and $|d_4| \le d_{4M}$.

Based on MLP technique, the controller u_{d} is designed as

$$\begin{aligned}u_{\mathrm{d}} = &-k_4 z_4 - \frac{1}{2} z_4 \hat{\varphi}_4 \Phi_4^T(\bar{x}, u_f)\Phi_4(\bar{x}, u_f) \\ &-\hat{d}_4 \tanh\left(\frac{z_4}{w_4}\right) + \dot{\varsigma}_{30} - z_3 - k_4\psi_1 \end{aligned} \tag{52}$$

where k_4 and w_4 are positive design constants. $\hat{d}_4 \tanh(z_4/w_4)$ is a robust compensator; $\hat{\varphi}_4$ and $\hat{d}_4$ denote the estimations of φ_4 and d_{4M}, respectively. $\hat{\varphi}_4$ and $\hat{d}_4$ are updated as

$$\dot{\hat{\varphi}}_4 = \frac{\rho_{41}}{2} z_4^2 \Phi_4^T(\bar{x}, u_f)\Phi_4(\bar{x}, u_f) - \sigma_{41}\hat{\varphi}_4 \tag{53}$$

$$\dot{\hat{d}}_4 = \rho_{42}\left[z_4 \tanh\left(\frac{z_4}{w_4}\right) - \sigma_{42}\hat{d}_4\right] \tag{54}$$

By substituting (52) into (51), (51) can be rewritten as

$$\begin{aligned}\dot{z}_4 = &-k_4 z_4 - z_3 + W_4^{*T}\Phi_4(\bar{x}, u_f) \\ &-\frac{1}{2} z_4 \hat{\varphi}_4 \Phi_4^T(\bar{x}, u_f)\Phi_4(\bar{x}, u_f) + d_4 - \hat{d}_4 \tanh\left(\frac{z_4}{w_4}\right) - \tau_3 \end{aligned} \tag{55}$$

The following theorem shows the design procedure and analysis of the modified BLF-based adaptive neural DSC for system (7) using back-stepping technique.

Theorem 2 *Consider the altitude subsystem* (7)*, under Assumption* 1*, control laws* (33), (39), (46), (52)*, updating laws* (34), (40), (41), (53), (54)*, and initial error condition* $|z_1(0)| < k_{b1}$*, then the closed-loop signals* $z_{i=1,2,3,4}$*,* $\tilde{\varphi}_{i=2,4}$*,* $\tilde{d}_{i=1,2,4}$ *are semi-globally bounded and the tracking error* z_1 *will remain in the compact set* $|z_1| < k_{b1}$.

Proof Please see "Appendix."

Remark 3 It should be mentioned that the MLP technique is used to estimate the maximum norm of the ideal weight vectors of RBFNN instead of their elements. Thus, the number of the online learning parameters is greatly reduced in the closed-loop system. On the basis of modified DSC and MLP technique, the control scheme can solve the problems of 'explosion of learning parameters' and 'explosion of complexity' simultaneously. Consequently, a much simpler controller with less computational load is obtained, which is better to be implemented in real applications. Additionally, it must be pointed out that the problems of the input saturation and output constraints are solved by employing an auxiliary system and the BLF, respectively.

Remark 4 Altitude subsystem (7) belongs to the system in pure-feedback form. Thus, the control designs and main conclusions could be naturally extended to the following pure-feedback system as given in [19]:

$$\begin{cases}\dot{x}_i = f_i(\bar{x}_i, x_{i+1}) + x_{i+1}, & i = 1, 2 \ldots n-1 \\ \dot{x}_n = f_n(\bar{x}_i, u) + u \end{cases} \tag{56}$$

where $\bar{x}_i = [x_1, x_2 \ldots x_i]$.

4 Simulations

In this section, simulation results are presented to illustrate the effectiveness of the modified adaptive neural control for longitudinal model of the morphing aircraft based on BLF. The aerodynamic coefficients and model parameters are the same as [2]. The scope of the input variables of NNs is defined as $V \in [0,\ 50\,\mathrm{m/s}]$, $\gamma \in [-10^\circ,\ 10^\circ]$, $\alpha \in [-10^\circ,\ 10^\circ]$ and $q \in [-15^\circ/\mathrm{s},\ 15^\circ/\mathrm{s}]$. The centers such as c_2, c_4 and c_V including 50 nodes are evenly spaced in their bounds. The widths of Gaussian functions are chosen as $b_{i2} = 2$, $b_{i4} = 5$, $b_{iV} = 4$. The initial conditions are set as $X_0 = [\gamma_0, \alpha_0, q_0, h_0, V_0] = [0^\circ, 0.99512^\circ, 0^\circ/\mathrm{s}, 1000\,\mathrm{m}, 30\,\mathrm{m/s}]$. Tracking error limits are set as $k_{b1} = 0.6$ and $k_{b2} = 0.2$. The control parameters and auxiliary compensation parameters are selected as $k_1 = 0.01$, $k_2 = 1.1$, $k_3 = 0.1$, $k_4 = 1.5$, $k_V = 10$. Gains for the adaptive laws are selected as $\rho_{12} = 1$, $\sigma_{12} = 0.1$, $\rho_{21} = 100$, $\sigma_{21} = 0.1$, $\rho_{22} = 10$, $\sigma_{22} = 0.1$, $\rho_{41} = 100$, $\sigma_{41} = 0.1$, $\rho_{42} = 100$, $\sigma_{42} = 0.1$, $\rho_{V1} = 2.5$, $\sigma_{V1} = 0.1$, $\rho_{V2} = 100$, $\sigma_{V2} = 0.1$, $w_{i=1,2,4,V} = 1$, $k_{22} = 1$. Reference commands are smoothened via several second-order filters which are given in (57).

$$\frac{h_{\mathrm{d}}}{h_{\mathrm{d}0}} = \frac{0.04}{s^2 + 0.4s + 0.04},\quad \frac{V_{\mathrm{d}}}{V_{\mathrm{d}0}} = \frac{0.04}{s^2 + 0.4s + 0.04},\quad \frac{\zeta_{\mathrm{d}}}{\zeta_{\mathrm{d}0}} = \frac{1}{s^2 + 2s + 1} \tag{57}$$

The following two scenarios are simulated to test the performance of the proposed controller in the presence of system uncertainty and input–output constraints.

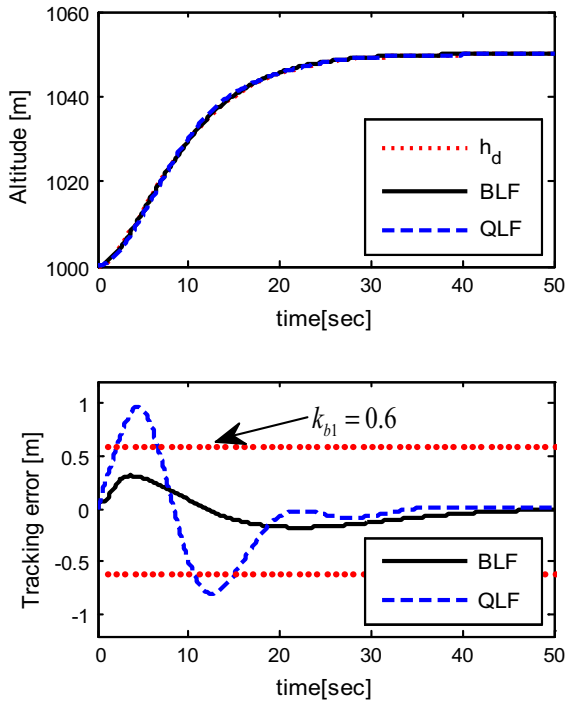

Fig. 2 Altitude tracking

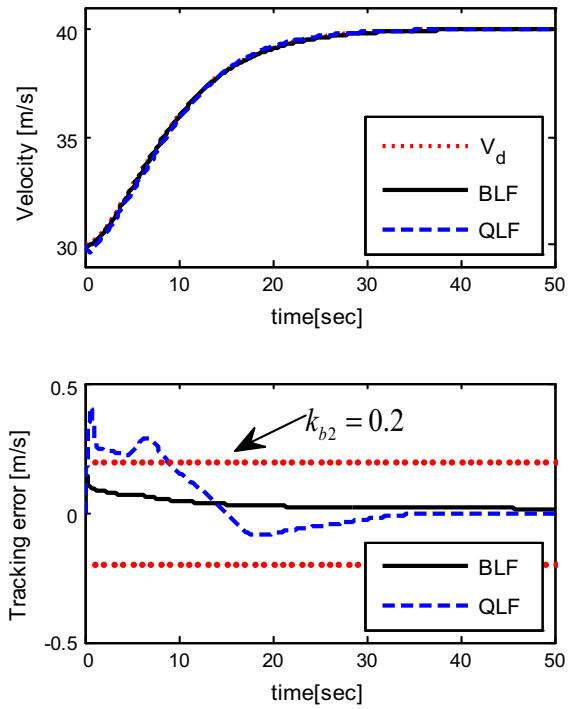

Fig. 3 Velocity tracking

Scenario 1 An adaptive back-stepping controller based on quadratic Lyapunov function (QLF) in [33] is compared to verify the proposed controller. We assume that the actuator saturation of control inputs is set as $\delta_e \in [-2°, 2°]$ and $T \in [0, 67]$N, respectively. The simulation results are depicted in Figs. 2, 3, 4, 5, 6 and 7. Figures 2 and 3 reveal that the BLF and QLF controllers achieve different tracking performance. The altitude and velocity tracking errors are within the compact set $|z_1| \leq 0.6$ and $|z_V| \leq 0.2$ when the BLF technique is used in the controller design. However, when the QLF controller is employed under the same initial conditions and control gains with BLF-based controller, the output constraints are violated. The response of control inputs and auxiliary variables is shown in Figs. 4 and 5. It is obvious to observe that the system inputs δ_e and T are both saturated and recover to normal with the compensation of auxiliary systems. Figures 6 and 7 show that the system states and $\hat{\varphi}_2$, $\hat{\varphi}_4$ and $\hat{\varphi}_V$ are bounded. Simulation results demonstrate that the system could achieve better tracking performance as compared to QLF-based controller.

Scenario 2 In this scenario, BLF-based adaptive neural controller is applied to the morphing aircraft's wing

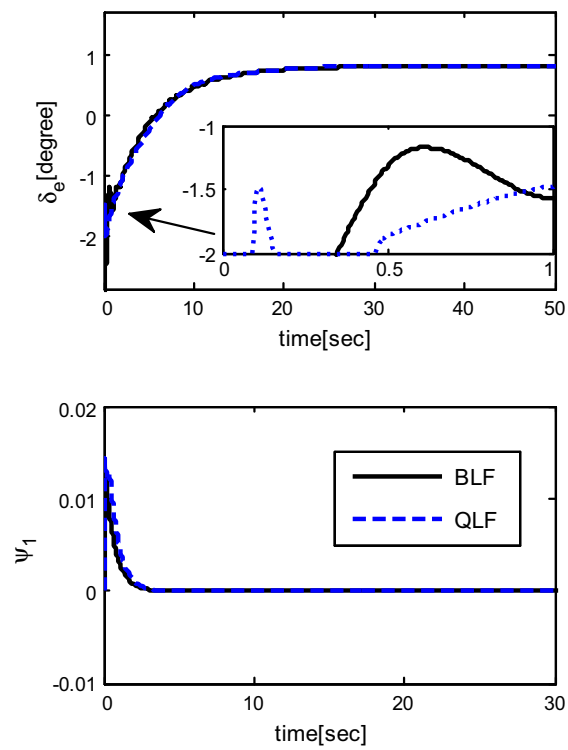

Fig. 4 Elevator deflection and ψ_1

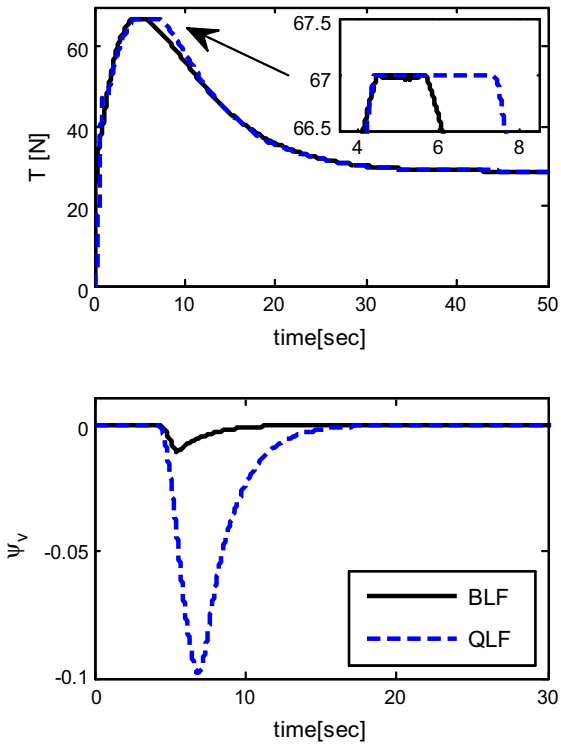

Fig. 5 Thrust and ψ_V

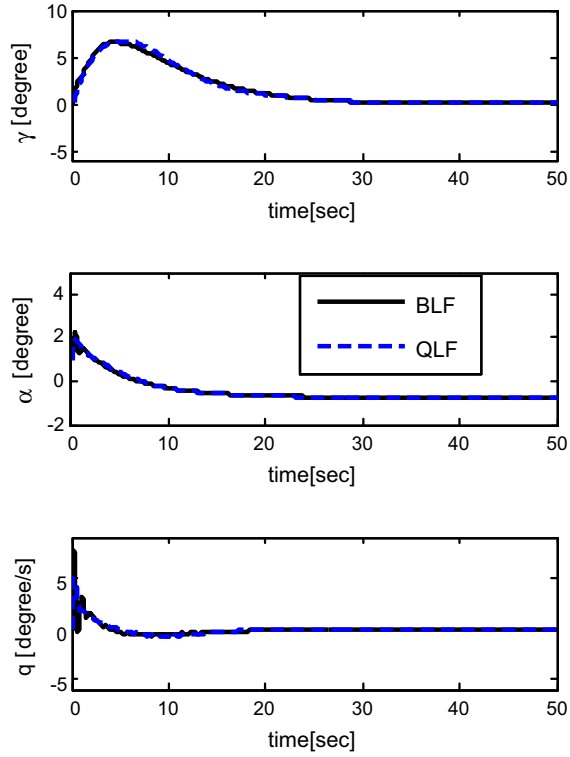

Fig. 6 System states

shape transition phase, while the actuator saturation of control inputs δ_e is released. The simulation results are shown in Figs. 8, 9, 10 and 11. From Fig. 10, it can be seen that the output velocity is nearly constant and altitude tracking error decreases about 0.2 m during the sweep process. The altitude and velocity tracking errors of BLF-based controller are not violated their boundaries k_{b1} and k_{b2}. After the wing finishes sweeping, the velocity and altitude errors converge within 20 s. However, the bound of velocity and altitude tracking errors for QLF controller are overstepped. From the curves of sweep reference signal ζ and system states (angle of attack, FPA and pitch rate) in Figs. 8 and 9, it can be observed that the angle of attack tends to reach a new equilibrium since the wing area decreases; meanwhile, other system states are bounded. In addition, as shown in Fig. 11, the changes in elevator defection and thrust are both within acceptable ranges. From the simulation results, it can be concluded that the BLF-based control scheme can accommodate different wing shapes and guarantee the steady flight.

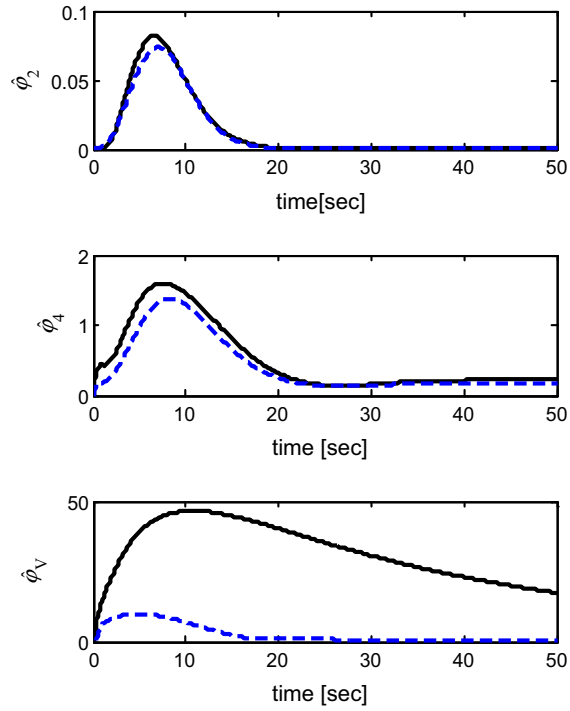

Fig. 7 Estimation of φ_2, φ_4 and φ_V

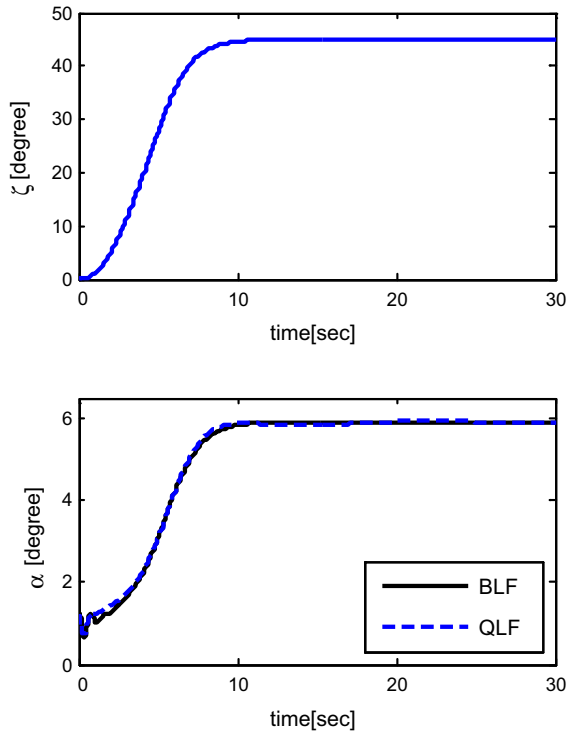

Fig. 8 Sweep reference signal and AOA

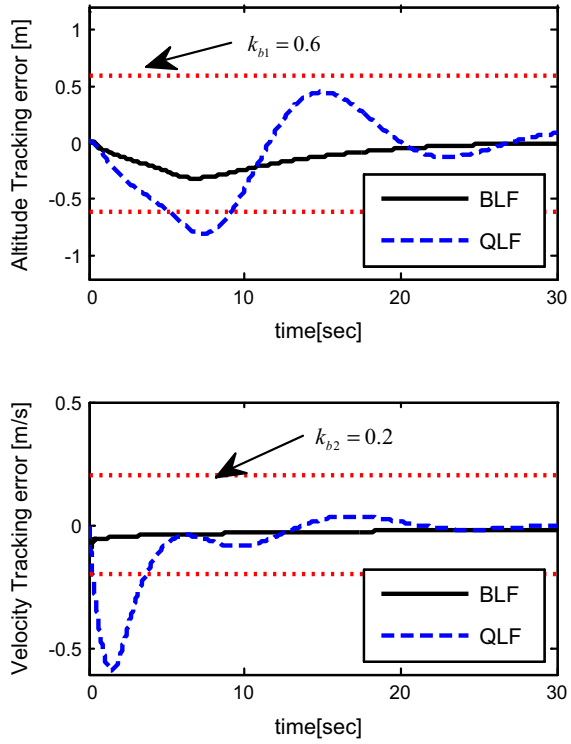

Fig. 10 Altitude and velocity variation

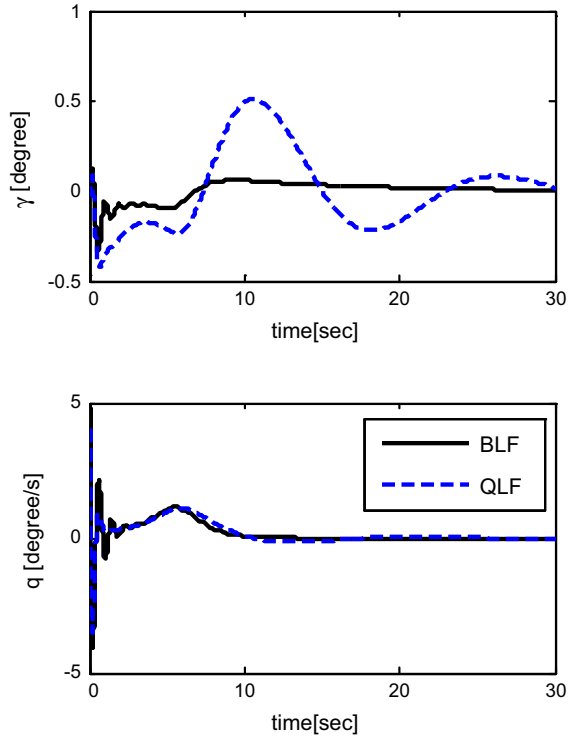

Fig. 9 FPA and pitch rate

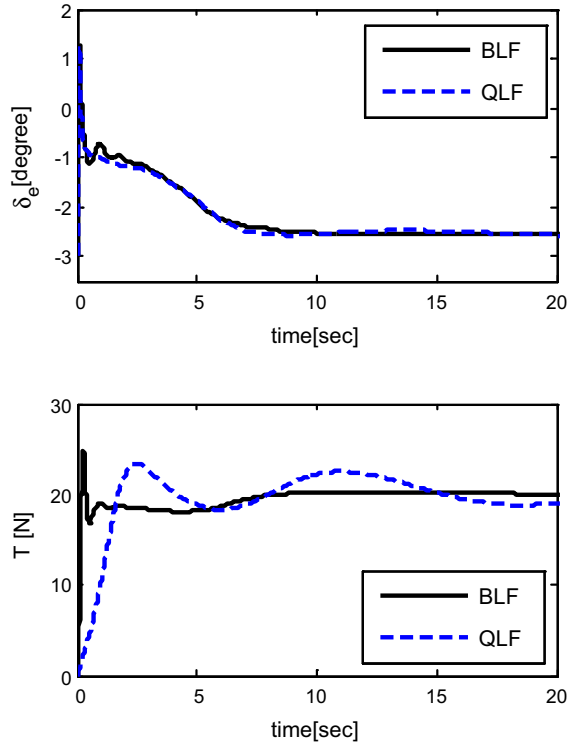

Fig. 11 Elevator deflection and thrust

5 Conclusions and future work

A modified adaptive neural dynamic surface control scheme is developed for morphing aircraft with unknown dynamics and input–output constraints. Minimal learning parameter technique-based neural networks are used to approximate the unknown system dynamics, thus solving the problem of 'explosion of learning parameter.' To overcome the inherent problem of 'explosion of complexity' in back-stepping design, the first-order sliding mode differentiator is applied to avoid the tedious analytic computation. Therefore, a barrier Lyapunov technique-based composite adaptive neural method, which is capable of dealing with input–output constraints and the problem of 'explosion of complexity' as well as 'explosion of NN's learning parameters,' is presented and a new type of adaptive laws is constructed by synthesizing the FOSD, MLP and auxiliary compensation system in the back-stepping design. Meanwhile, this control scheme can be further extended to control a class of nonlinear system in pure-feedback form. Comparative results verify the superiority of the proposed controller.

In the future work, the authors will focus on the problem of the unmeasured states and disturbance observer [50] in the control design based on adaptive neural DSC scheme.

Acknowledgements The authors would like to express their sincere thanks to anonymous reviewers for their helpful suggestions for improving the technique note. This work is partially supported by the Natural Science Foundation of China (Grant Nos. 61374032, 61573286), Aeronautical Science Foundation of China (Grant No. 20140753012).

Appendix

Proof of Theorem 1

Proof Considering the following candidate Lyapunov function

$$L_V = \frac{1}{2}\log\left(\frac{k_{b2}^2}{k_{b2}^2 - z_V^2}\right) + \frac{1}{2\rho_{V1}}\tilde{\varphi}_V^2 + \frac{1}{2\rho_{V2}}\tilde{d}_V^2 \tag{58}$$

where ρ_{V1} and ρ_{V2} are positive design parameters, $\tilde{\varphi}_V = \varphi_V - \hat{\varphi}_V$ and $\tilde{d}_V = d_{VM} - \hat{d}_V$.

Based on (25), (26) and (27), the time derivative of L_V is given by

$$\begin{aligned}\dot{L}_V = {} & \frac{z_V \dot{z}_V}{k_{b2}^2 - z_V^2} - \frac{1}{\rho_{V1}}\tilde{\varphi}_V\dot{\hat{\varphi}}_V - \frac{1}{\rho_{V2}}\tilde{d}_V\dot{\hat{d}}_V = \frac{z_V}{k_{b2}^2 - z_V^2}\begin{bmatrix} -k_V z_V - \frac{z_V \hat{\varphi}_V \Phi_V^T(\bar{x}_V, T_f)\Phi_V(\bar{x}_V, T_f)}{4(k_{b2}^2 - z_V^2)k_{22}} + d_V + W_V^{*T}\Phi_V(\bar{x}_V, T_f) \\ -\hat{d}_V \tanh\left[\frac{z_V}{k_{b2}^2 - z_V^2}\frac{1}{w_V}\right] \end{bmatrix} \\ & - \tilde{\varphi}_V\left[\frac{z_V^2 \Phi_V^T(\bar{x}_V, T_f)\Phi_V(\bar{x}_V, T_f)}{4(k_{b2}^2 - z_V^2)^2 k_{22}} - \frac{\sigma_{V1}}{\rho_{V1}}\hat{\varphi}_V\right] - \tilde{d}_V\left[\frac{z_V}{k_{b2}^2 - z_V^2}\tanh\left(\frac{z_V}{k_{b2}^2 - z_V^2}\frac{1}{w_V}\right) - \sigma_{V2}\hat{d}_V\right]\end{aligned} \tag{59}$$

Note that the following inequalities hold

$$\begin{aligned}& \frac{z_V}{k_{b2}^2 - z_V^2} W_V^{*T}\Phi_V^T(\bar{x}_V, T_f) \\ & \quad \le \frac{\varphi_V z_V^2 \Phi_V^T(\bar{x}_V, T_f)\Phi_V(\bar{x}_V, T_f)}{4(k_{b2}^2 - z_V^2)^2 k_{22}} + k_{22}\end{aligned} \tag{60}$$

$$\begin{aligned}& \left|\frac{z_V}{k_{b2}^2 - z_V^2}\right| d_{VM} - \frac{z_V}{k_{b2}^2 - z_V^2} d_{VM}\tanh\left(\frac{z_V}{k_{b2}^2 - z_V^2}\frac{1}{w_V}\right) \\ & \quad \le \kappa_0 d_{VM} w_V = \bar{w}_V\end{aligned} \tag{61}$$

where $k_{22} > 0$.

Invoking $\tilde{\varphi}_V = \varphi_V - \hat{\varphi}_V$ and $\tilde{d}_V = d_{VM} - \hat{d}_V$ yields

$$\begin{aligned}\frac{\sigma_{V1}}{\rho_{V1}}\tilde{\varphi}_V\hat{\varphi}_V &= \frac{\sigma_{V1}}{2\rho_{V1}}\left(\varphi_V^2 - \tilde{\varphi}_V^2 - \hat{\varphi}_V^2\right) \\ &\le \frac{\sigma_{V1}}{2\rho_V}\left(\varphi_V^2 - \tilde{\varphi}_V^2\right), \\ \sigma_{V2}\tilde{d}_V\hat{d}_V &\le \frac{\sigma_{V2}}{2}\left(d_{VM}^2 - \tilde{d}_V^2\right)\end{aligned} \tag{62}$$

Consider that (60), (61), (62) and Lemma 3, (59) can be re-formulated as

$$\begin{aligned}\dot{L}_V &\le -\frac{k_V z_V^2}{k_{b2}^2 - z_V^2} - \frac{\sigma_{V1}}{2\rho_{V1}}\tilde{\varphi}_V^2 - \frac{\sigma_{V2}}{2}\tilde{d}_V^2 + \frac{\sigma_{V1}}{2\rho_{V1}}\varphi_V^2 \\ &\quad + \frac{\sigma_{V2}}{2}d_{VM}^2 + \bar{w}_V + k_{22} \\ &\le -k_V \log\frac{k_{b2}^2}{k_{b2}^2 - z_V^2} - \frac{\sigma_{V1}}{2\rho_{V1}}\tilde{\varphi}_V^2 \\ &\quad - \frac{\sigma_{V2}}{2}\tilde{d}_V^2 + C_{2V} \le -C_{1V}L_V + C_{2V}\end{aligned} \tag{63}$$

where $C_{1V} = \min\{2k_V, \sigma_{V1}/\rho_{V1}, \sigma_{V2}\}$, $C_{V2} = \frac{\sigma_{V1}}{2\rho_{V1}}\varphi_V^2 + \frac{\sigma_{V2}}{2}d_{VM}^2 + \bar{w}_V + k_{22}$.

Multiplying (63) by $e^{C_{V1}t}$, we have

$$\frac{\mathrm{d}}{\mathrm{d}t}(L_V e^{C_{V1}t}) \leq C_{V2} e^{C_{V1}t} \tag{64}$$

Integrating the above inequality, we obtain

$$L_V \leq (L_V(0) - \frac{C_{V2}}{C_{V1}})e^{-C_{V1}t} + \frac{C_{V2}}{C_{V1}} \tag{65}$$

Therefore, for z_V we obtain

$$\frac{1}{2}\log\left(\frac{k_{b2}^2}{k_{b2}^2 - z_V^2}\right) \leq L_V(0) + \frac{C_{V2}}{C_{V1}},$$
$$|z_V| \leq k_{b2}\sqrt{(1 - e^{-2(L_V(0)+C_{V2}/C_{V1})})} < k_{b2} \tag{66}$$

Similarly, we have $|\tilde{\varphi}_V| \leq \sqrt{2\rho_{V1}(L_V(0) + C_{V2}/C_{V1})}$, $\left|\tilde{d}_V\right| \leq \sqrt{2\rho_{V2}(L_V(0) + C_{V2}/C_{V1})}$.

Proof of Theorem 2

Proof Choose the following candidate Lyapunov function

$$L = L_1 + L_2 + L_3 + L_4 \tag{67}$$

where $L_1 = \frac{1}{2V}\log\left(\frac{k_{b1}^2}{k_{b1}^2 - z_1^2}\right) + \frac{1}{2\rho_{12}}\tilde{d}_1^2$, $L_2 = \frac{1}{2}z_2^2 + \frac{\tilde{\varphi}_2^2}{2\rho_{21}} + \frac{\tilde{d}_2^2}{2\rho_{22}}$, $L_3 = \frac{1}{2}z_3^2$, $L_4 = \frac{1}{2}z_4^2 + \frac{\tilde{\varphi}_4^2}{2\rho_{41}} + \frac{\tilde{d}_4^2}{2\rho_{42}}$, and $\tilde{d}_1 = d_{1M} - \hat{d}_1$, $\tilde{\varphi}_2 = \varphi_2 - \hat{\varphi}_2$, $\tilde{d}_2 = d_{2M} - \hat{d}_2$, $\tilde{\varphi}_4 = \varphi_4 - \hat{\varphi}_4$, $\tilde{d}_4 = d_{4M} - \hat{d}_4$.

According to (34), (35) and Lemma 2, the time derivative of L_1 is given by

$$\begin{aligned}
\dot{L}_1 &= \frac{1}{V}\frac{z_1\dot{z}_1}{k_{b1}^2 - z_1^2} - \frac{\dot{V}}{2V^2}\log\frac{k_{b1}^2}{k_{b1}^2 - z_1^2} - \frac{1}{\rho_{12}}\tilde{d}_1\dot{\hat{d}}_1 \\
&= \frac{z_1}{k_{b1}^2 - z_1^2}\left(z_2 - k_1 z_1 - \frac{z_1}{2(k_{b1}^2 - z_1^2)}\right. \\
&\quad \left. - z_1\hat{d}_1\tanh\left(\frac{z_1^2}{k_{b1}^2 - z_1^2}\frac{1}{w_1}\right)\right) \\
&\quad + d_1\log\frac{k_{b1}^2}{k_{b1}^2 - z_1^2} - \frac{1}{\rho_{12}}\tilde{d}_1\dot{\hat{d}}_1 \\
&\leq -\frac{k_1 z_1^2}{k_{b1}^2 - z_1^2} + \frac{z_1 z_2}{k_{b1}^2 - z_1^2} - \frac{z_1^2}{2(k_{b1}^2 - z_1^2)^2} \\
&\quad + \left|d_{1M}\frac{z_1^2}{k_{b1}^2 - z_1^2}\right| - d_{1M}\frac{z_1^2}{k_{b1}^2 - z_1^2}\tanh\left(\frac{z_1^2}{k_{b1}^2 - z_1^2}\frac{1}{w_1}\right) \\
&\quad + \sigma_{12}\tilde{d}_1\hat{d}_1
\end{aligned} \tag{68}$$

By invoking (40), (41), (42), the time derivative of L_2 is given by

$$\begin{aligned}
\dot{L}_2 &= z_2\dot{z}_2 - \frac{1}{\rho_{21}}\tilde{\varphi}_2\dot{\hat{\varphi}}_2 - \frac{1}{\rho_{22}}\tilde{d}_2\dot{\hat{d}}_2 \\
&\leq z_2 z_3 - k_2 z_2^2 + z_2 W_2^{*T}\Phi_2(x_2, x_{3f}) \\
&\quad - \frac{1}{2}\varphi_2 z_2^2\Phi_2^T(x_2, x_{3f})\Phi_2(x_2, x_{3f}) \\
&\quad + |z_2|\, d_{2M} - z_2 d_{2M}\tanh\left(\frac{z_2}{w_2}\right) - z_2\tau_1 \\
&\quad + \frac{\sigma_{21}}{\rho_{21}}\tilde{\varphi}_2\hat{\varphi}_2 + \sigma_{22}\tilde{d}_2\hat{d}_2
\end{aligned} \tag{69}$$

Considering (47) and (48), the time derivative of L_3 is obtained as

$$\begin{aligned}
\dot{L}_3 &= z_3\dot{z}_3 = z_3(z_4 - z_2 - k_3 z_3 - \tau_2) \\
&\leq -\left(k_3 - \frac{1}{2k_{11}}\right)z_3^2 - z_2 z_3 + z_3 z_4 + \frac{k_{11}}{2}\bar{\tau}_2^2
\end{aligned} \tag{70}$$

Using (53), (54) and (55) results in the time derivative of L_4

$$\begin{aligned}
\dot{L}_4 &= z_4\dot{z}_4 - \frac{1}{\rho_{41}}\tilde{\varphi}_4\dot{\hat{\varphi}}_4 - \frac{1}{\rho_{42}}\tilde{d}_4\dot{\hat{d}}_4 \\
&= z_4\left(-k_4 z_4 - z_3 + W_4^{*T}\Phi_4(\bar{x}, u_f)\right. \\
&\quad - \frac{1}{2}z_4\hat{\varphi}_4\Phi_4^T(\bar{x}, u_f)\Phi_4(\bar{x}, u_f) + d_4 \\
&\quad \left. - \hat{d}_4\tanh\left(\frac{z_4}{w_4}\right) - \tau_3\right) \\
&\quad - \frac{1}{\rho_{41}}\tilde{\varphi}_4\dot{\hat{\varphi}}_4 - \frac{1}{\rho_{42}}\tilde{d}_4\dot{\hat{d}}_4 \\
&\leq -k_4 z_4^2 - z_3 z_4 + z_4 W_4^{*T}\Phi_4(\bar{x}, u_f) \\
&\quad - \frac{1}{2}z_4^2\varphi_4\Phi_4^T(\bar{x}, u_f)\Phi_4(\bar{x}, u_f) + |z_4|\, d_{4M} \\
&\quad - z_4 d_{4M}\tanh\left(\frac{z_4}{w_4}\right) - z_4\tau_3 + \frac{1}{\rho_{41}}\tilde{\varphi}_4\hat{\varphi}_4 + \frac{1}{\rho_{42}}\tilde{d}_4\hat{d}_4
\end{aligned} \tag{71}$$

Consider the following facts

$$\sigma_{12}\tilde{d}_1\hat{d}_1 \le \frac{\sigma_{12}}{2}\left(d_{1M}^2-\tilde{d}_1^2\right),\quad \frac{z_1z_2}{k_{b1}^2-z_1^2} \le \frac{z_1^2}{2(k_{b1}^2-z_1^2)^2}+\frac{1}{2}z_2^2,\quad -z_2\tau_1 \le \frac{1}{2}z_2^2+\frac{1}{2}\bar{\tau}_1^2 \tag{72}$$

$$d_{1M}\left|\frac{z_1^2}{k_{b1}^2-z_1^2}\right|-d_{1M}\frac{z_1^2}{k_{b1}^2-z_1^2}\tanh\left(\frac{z_1^2}{k_{b1}^2-z_1^2}\frac{1}{w_1}\right) \le \kappa_0 d_{1M}w_1=\bar{w}_1,$$

$$\frac{\sigma_{21}}{\rho_{21}}\tilde{\varphi}_2\hat{\varphi}_2 \le \frac{\sigma_{21}}{2\rho_{21}}\varphi_2^2-\frac{\sigma_{21}}{2\rho_{21}}\tilde{\varphi}_2^2 \tag{73}$$

$$|z_2|\,d_{2M}-z_2d_{2M}\tanh\left(\frac{z_2}{w_2}\right) \le \kappa_0 d_{2M}w_2=\bar{w}_2,$$

$$\sigma_{22}\tilde{d}_2\hat{d}_2 \le \frac{1}{2}\sigma_{22}d_{2M}^2-\frac{1}{2}\sigma_{22}\tilde{d}_2^2 \tag{74}$$

$$z_2W_2^{*T}\Phi(\bar{x},u_f) \le \frac{1}{2}z_2^2\varphi_2\Phi_2^T(\bar{x},u_f)\Phi_2(\bar{x},u_f)+\frac{1}{2},$$

$$\frac{\sigma_{41}}{\rho_{41}}\tilde{\varphi}_4\hat{\varphi}_4 \le \frac{\sigma_{41}}{2\rho_{41}}\left(\varphi_4^2-\tilde{\varphi}_4^2\right) \tag{75}$$

$$-z_4\tau_3 \le \frac{1}{2}\left(z_4^2+\bar{\tau}_3^2\right),$$

$$|z_4|\,d_{4M}-z_4d_{4M}\tanh\left(\frac{z_4}{w_4}\right) \le \kappa_0 d_{4M}w_4=\bar{w}_4 \tag{76}$$

$$\sigma_{42}\tilde{d}_4\hat{d}_4 \le \frac{1}{2}\sigma_{42}\left(d_{4M}^2-\tilde{d}_4^2\right),$$

$$z_4W_4^{*T}\Phi(\bar{x},u_f) \le \frac{1}{2}z_4^2\varphi_4\Phi_4^T(\bar{x},u_f)\Phi_4(\bar{x},u_f)+\frac{1}{2} \tag{77}$$

The derivative of L is obtained as

$$\begin{aligned}\dot{L}&=\dot{L}_1+\dot{L}_2+\dot{L}_3+\dot{L}_4\\ &\le -k_1\log\frac{k_{b1}^2}{k_{b1}^2-z_1^2}-(k_2-1)z_2^2-\left(k_3-\frac{1}{2k_{11}}\right)z_3^2\\ &\quad-(k_4-0.5)z_4^2-\frac{\sigma_{12}}{2}\tilde{d}_1^2-\frac{\sigma_{21}}{2\rho_{21}}\tilde{\varphi}_2^2\\ &\quad-\frac{\sigma_{22}}{2}\tilde{d}_2^2-\frac{\sigma_{41}}{2\rho_{41}}\tilde{\varphi}_4^2-\frac{\sigma_{42}}{2}\tilde{d}_4^2+\frac{\sigma_{12}}{2}d_{1M}^2+\frac{\sigma_{22}}{2}d_{2M}^2\\ &\quad+\frac{\sigma_{42}}{2}d_{4M}^2+\frac{\sigma_{21}}{2\rho_{21}}\varphi_2^2\\ &\quad+\frac{\sigma_{41}}{2\rho_{41}}\varphi_4^2+\bar{w}_1+\bar{w}_2+\bar{w}_4+\frac{1}{2}\bar{\tau}_1^2+\frac{k_{11}}{2}\bar{\tau}_2^2\\ &\quad+\frac{1}{2}\bar{\tau}_3^2+1\ \le -C_1L+C_2\end{aligned} \tag{78}$$

where $C_1 := \left(2k_1, 2k_2-2, 2k_3-\frac{1}{k_{11}}, 2k_4-1, \sigma_{12}, \frac{\sigma_{21}}{\rho_{21}}, \sigma_{22}, \frac{\sigma_{41}}{\rho_{41}}, \sigma_{42}\right)$,

$$C_2 := \begin{pmatrix}0.5\sigma_{12}d_{1M}^2+0.5\sigma_{22}d_{2M}^2+0.5\sigma_{42}d_{4M}^2+0.5\sigma_{21}/\rho_{21}\varphi_2^2+0.5\sigma_{41}/\rho_{41}\varphi_4^2+\bar{w}_1+\bar{w}_2+\bar{w}_4\\ +0.5\bar{\tau}_1^2+0.5k_{11}\bar{\tau}_2^2+0.5\bar{\tau}_3^2+1\end{pmatrix}.$$

To ensure $C_1>0$, the corresponding design parameters $k_{i=1,2,3,4}$, $\sigma_{ij,i=1,2,4,j=1,2}$ and $\rho_{ij,i=1,2,3,j=1,2}$ should be chosen such that $k_1>0$, $k_2-1>0$, $k_3-0.5/k_{11}>0$, $k_4-0.5>0$, $\sigma_{ij,i=1,2,3,j=1,2}>0$ and $\rho_{ij,i=1,2,4,j=1,}>0$. Multiplying (78) by e^{C_1t}, we can get $\frac{\mathrm{d}}{\mathrm{d}t}(Le^{C_1t}) \le C_2e^{C_1t}$. Integrating inequality $\frac{\mathrm{d}}{\mathrm{d}t}(Le^{C_1t}) \le C_2e^{C_1t}$, we obtain

$$L \le (L(0)-\frac{C_2}{C_1})e^{-C_1t}+\frac{C_2}{C_1} \tag{79}$$

Therefore, we have

$$\frac{1}{2}\log\left(\frac{k_{b1}^2}{k_{b1}^2-z_1^2}\right) \le L(0)+\frac{C_2}{C_1},\qquad |z_1| \le k_{b1}\sqrt{(1-e^{-2(L(0)+C_2/C_1)})} < k_{b1} \tag{80}$$

Similarly, we obtain

$$\begin{aligned}&|z_2| \le \sqrt{2(L(0)+C_2/C_1)},\\ &|z_3| \le \sqrt{2(L(0)+C_2/C_1)},\\ &|z_4| \le \sqrt{2(L(0)+C_2/C_1)},\\ &\left|\tilde{d}_1\right| \le \sqrt{2\rho_{12}(L(0)+C_2/C_1)},\\ &|\tilde{\varphi}_2| \le \sqrt{2\rho_{21}(L(0)+C_2/C_1)},\\ &\left|\tilde{d}_2\right| \le \sqrt{2\rho_{22}(L(0)+C_2/C_1)},\\ &|\tilde{\varphi}_4| \le \sqrt{2\rho_{41}(L(0)+C_2/C_1)},\\ &\left|\tilde{d}_4\right| \le \sqrt{2\rho_{42}(L(0)+C_2/C_1)}.\end{aligned}$$

References

1. Shi, R., Peng, J.: Morphing strategy design for variable wing aircraft. In: 15th AIAA Aciation Technology, Integration, and Operations Conference, Dallas, TX (2015)
2. Wu, Z., Lu, J., Rajput, J., Shi, J., Ma, W.: Adaptive neural control based on high order integral chained differentiator for morphing aircraft. Math. Probl. Eng. (2015). doi:10.1155/2015/787931
3. Seigler, T.M., Neal, D.A., Bae, J.-S., Inman, D.J.: Modeling and flight control of large-scale morphing aircraft. J. Aircr. **44**(4), 1077–1087 (2007). doi:10.2514/1.21439
4. Baldelli, D.H., Lee, D.-H., Sánchez Peña, R.S., Cannon, B.: Modeling and control of an aeroelastic morphing vehicle. J. Guid. Control Dyn. **31**(6), 1687–1699 (2008). doi:10.2514/1.35445
5. Yue, T., Wang, L., Ai, J.: Gain self-scheduled H∞ control for morphing aircraft in the wing transition process based on an LPV model. Chin. J. Aeronaut. **26**(4), 909–917 (2013)
6. Wang, T., Dong, C., Wang, Q.: Finite-time boundedness control of morphing aircraft based on switched systems approach. Opt. Int. J. Light Electron Opt. **126**(23), 4436–4445 (2015). doi:10.1016/j.ijleo.2015.08.040
7. Jiang, W., Dong, C., Wang, Q.: A systematic method of smooth switching LPV controllers design for a morphing aircraft. Chin. J. Aeronaut. **28**(6), 1640–1649 (2015). doi:10.1016/j.cja.2015.10.005
8. Wang, N., Qian, C., Sun, J.C., Liu, Y.C.: Adaptive robust finite-time trajectory tracking control of fully actuated marine surface vehicles. IEEE Trans. Control Syst. Technol. **24**(4), 1454–1462 (2016). doi:10.1109/TCST.2015.2496585
9. Nikdel, N., Badamchizadeh, M., Azimirad, V., Nazari, M.A.: Fractional-order adaptive backstepping control of robotic manipulators in the presence of model uncertainties and external disturbances. IEEE Trans. Ind. Electron. **63**(10), 6249–6256 (2016). doi:10.1109/TIE.2016.2577624
10. Aggarwal, A., Kumar, M., Rawat, T.K., Upadhyay, D.K.: Optimal design of 2D FIR filters with quadrantally symmetric properties using fractional derivative constraints. Circuits Syst. Signal Process. **35**(6), 2213–2257 (2016). doi:10.1007/s00034-016-0283-x
11. Kumar, M., Rawat, T.K.: Fractional order digital differentiator design based on power function and least squares. Int. J. Electron. (2016). doi:10.1080/00207217.2016.1138520
12. Kumar, M., Rawat, T.K.: Design of a variable fractional delay filter using comprehensive least square method encompassing all delay values. J. Circuits Syst. Comput. (2015). doi:10.1142/S0218126615501169
13. Aggarwal, A., Rawat, T.K., Kumar, M., Upadhyay, D.K.: Efficient design of digital FIR differentiator using L1-method. Radioengineering **25**(2), 86–92 (2016)
14. Yixin, D., Passino, K.M.: Adaptive neural/fuzzy control for interpolated nonlinear systems. IEEE Trans. Fuzzy Syst. **10**(5), 583–595 (2002). doi:10.1109/tfuzz.2002.803493
15. Tong, S., Zhang, L., Li, Y.: Observed-based adaptive fuzzy decentralized tracking control for switched uncertain nonlinear large-scale systems with dead zones. IEEE Trans. Syst. Man Cybern. Syst. **46**(1), 37–47 (2016). doi:10.1109/tsmc.2015.2426131
16. Wang, N., Er, M.J.: Self-constructing adaptive robust fuzzy neural tracking control of surface vehicles with uncertainties and unknown disturbances. IEEE Trans. Control Syst. Technol. **23**(3), 991–1002 (2015). doi:10.1109/TCST.2014.2359880
17. Wang, N., Er, M.J.: Direct adaptive fuzzy tracking control of marine vehicles with fully unknown parametric dynamics and uncertainties. IEEE Trans. Control Syst. Technol. **24**(5), 1845–1852 (2016). doi:10.1109/TCST.2015.2510587
18. Wang, N., Er, M.J., Sun, J.C., Liu, Y.C.: Adaptive robust online constructive fuzzy control of a complex surface vehicle system. IEEE Trans. Cybern. **46**(7), 1511–1523 (2016). doi:10.1109/TCYB.2015.2451116
19. An Min, Z., Zeng Guang, H., Min, T.: Adaptive control of a class of nonlinear pure feedback systems using fuzzy backstepping approach. IEEE Trans. Fuzzy Syst. **16**(4), 886–897 (2008)
20. Qi, Z., Peng, S., Jinjun, L., Shengyuan, X.: Adaptive output-feedback fuzzy tracking control for a class of nonlinear systems. IEEE Trans. Fuzzy Syst. **19**(5), 972–982 (2011). doi:10.1109/tfuzz.2011.2158652
21. Li, Y., Tong, S.: Adaptive fuzzy output-feedback control of pure-feedback uncertain nonlinear systems with unknown dead zone. IEEE Trans. Fuzzy Syst. **22**(5), 1341–1347 (2014). doi:10.1109/tfuzz.2013.2280146
22. Li, T.S., Wang, D., Feng, G., Tong, S.C.: A DSC approach to robust adaptive NN tracking control for strict-feedback nonlinear systems. IEEE Trans. Syst. Man Cybern. **40**(3), 915–927 (2010). doi:10.1109/TSMCB.2009.2033563
23. Yoo, S.J.: Adaptive output-feedback control for nonlinear time-delay systems in pure-feedback form. J. Frankl. Inst. **351**(7), 3899–3913 (2014). doi:10.1016/j.jfranklin.2014.04.003
24. Wang, Y., Wu, H.: Adaptive robust backstepping control for a class of uncertain dynamical systems using neural networks. Nonlinear Dyn. **81**(4), 1597–1610 (2015). doi:10.1007/s11071-015-2093-2
25. Jiang, B., Shen, Q., Shi, P.: Neural-networked adaptive tracking control for switched nonlinear pure-feedback systems under arbitrary switching. Automatica **61**, 119–125 (2015). doi:10.1016/j.automatica.2015.08.001
26. Xu, B., Yang, C., Pan, Y.: Global neural dynamic surface tracking control of strict-feedback systems with application to hypersonic flight vehicle. IEEE Trans. Neural Netw. Learn Syst. **26**(10), 2563–2575 (2015). doi:10.1109/TNNLS.2015.2456972
27. Xu, B.: Robust adaptive neural control of flexible hypersonic flight vehicle with dead-zone input nonlinearity. Nonlinear Dyn. **80**(3), 1509–1520 (2015). doi:10.1007/s11071-015-1958-8
28. Xu, B., Shi, Z., Yang, C., Sun, F.: Composite neural dynamic surface control of a class of uncertain nonlinear systems in strict-feedback form. IEEE Trans. Cybern. **44**(12), 2626–2634 (2014). doi:10.1109/TCYB.2014.2311824
29. He, W., Ge, S.S.: Vibration control of a flexible string with both boundary input and output constraints. IEEE Trans. Control Syst. Technol. **23**(4), 1245–1254 (2015). doi:10.1109/TCST.2014.2362718
30. Chen, M., Ge, S.S., Ren, B.: Adaptive tracking control of uncertain MIMO nonlinear systems with input con-

straints. Automatica **47**(3), 452–465 (2011). doi:10.1016/j.automatica.2011.01.025
31. Chen, M., Tao, G., Jiang, B.: Dynamic surface control using neural networks for a class of uncertain nonlinear systems with input saturation. IEEE Trans. Neural Netw. Learn. Syst. **26**(9), 2086–2097 (2015). doi:10.1109/TNNLS.2014.2360933
32. Li, Y., Tong, S., Li, T.: Composite adaptive fuzzy output feedback control design for uncertain nonlinear strict-feedback systems with input saturation. IEEE Trans. Cybern. **45**(10), 2299–2308 (2015). doi:10.1109/TCYB.2014.2370645
33. Zong, Q., Wang, F., Tian, B., Su, R.: Robust adaptive dynamic surface control design for a flexible air-breathing hypersonic vehicle with input constraints and uncertainty. Nonlinear Dyn. **78**(1), 289–315 (2014). doi:10.1007/s11071-014-1440-z
34. Bu, X., Wu, X., Ma, Z., Zhang, R., Huang, J.: Novel auxiliary error compensation design for the adaptive neural control of a constrained flexible air-breathing hypersonic vehicle. Neurocomputing **171**, 313–324 (2016). doi:10.1016/j.neucom.2015.06.058
35. Tee, K.P., Ge, S.S., Tay, E.H.: Barrier Lyapunov functions for the control of output-constrained nonlinear systems. Automatica **45**(4), 918–927 (2009). doi:10.1016/j.automatica.2008.11.017
36. Ren, B., Ge, S.S., Tee, K.P., Lee, T.H.: Adaptive neural control for output feedback nonlinear systems using a barrier Lyapunov function. IEEE Trans. Neural Netw. **21**(8), 1339–1345 (2010). doi:10.1109/TNN.2010.2047115
37. Liu, Y., Li, J., Tong, S., Chen, C.L.P.: Neural network control-based adaptive learning design for nonlinear systems with full-state constraints. IEEE Trans. Neural Netw. Learn. Syst. (2016). doi:10.1109/TNNLS.2015.2508926
38. Zhai, D., An, L., Li, J., Zhang, Q.: Simplified filtering-based adaptive fuzzy dynamic surface control approach for nonlinear strict-feedback systems. IET Control Theory Appl. **10**(5), 493–503 (2016). doi:10.1049/iet-cta.2015.0264
39. Liu, Y.-J., Tong, S.: Barrier Lyapunov functions-based adaptive control for a class of nonlinear pure-feedback systems with full state constraints. Automatica **64**, 70–75 (2016). doi:10.1016/j.automatica.2015.10.034
40. Kim, B.S., Yoo, S.J.: Approximation-based adaptive tracking control of nonlinear pure-feedback systems with time-varying output constraints. Int. J. Control Autom. Syst. **13**(2), 257–265 (2014). doi:10.1007/s12555-014-0084-6
41. Kim, B.S., Yoo, S.J.: Adaptive control of nonlinear pure-feedback systems with output constraints: integral barrier Lyapunov functional approach. Int. J. Control Autom. Syst. **13**(1), 249–256 (2014). doi:10.1007/s12555-014-0018-3
42. Gao, Y., Tong, S., Li, Y.: Observer-based adaptive fuzzy output constrained control for MIMO nonlinear systems with unknown control directions. Fuzzy Sets Syst. **290**, 79–99 (2016). doi:10.1016/j.fss.2015.04.005
43. Meng, W., Yang, Q., Sun, Y.: Adaptive neural control of nonlinear MIMO systems with time-varying output constraints. IEEE Trans. Neural Netw. Learn. Syst. **26**(5), 1074–1085 (2015). doi:10.1109/TNNLS.2014.2333878
44. Liu, Z., Lai, G., Zhang, Y., Chen, C.L.: Adaptive neural output feedback control of output-constrained nonlinear systems with unknown output nonlinearity. IEEE Trans. Neural Netw. Learn. Syst. **26**(8), 1789–1802 (2015). doi:10.1109/TNNLS.2015.2420661
45. He, W., Zhang, S., Ge, S.S.: Adaptive control of a flexible crane system with the boundary output constraint. IEEE Trans. Ind. Electron. **61**(8), 4126–4133 (2014). doi:10.1109/tie.2013.2288200
46. He, W., Chen, Y., Yin, Z.: Adaptive neural network control of an uncertain robot with full-state constraints. IEEE Trans. Cybern. **46**(3), 620–629 (2016). doi:10.1109/TCYB.2015.2411285
47. Li, Y., Li, T., Jing, X.: Indirect adaptive fuzzy control for input and output constrained nonlinear systems using a barrier Lyapunov function. Int. J. Adapt. Control Signal Process. **28**(2), 184–199 (2014). doi:10.1002/acs.2410
48. Li, Y., Tong, S., Li, T.: Adaptive fuzzy output-feedback control for output constrained nonlinear systems in the presence of input saturation. Fuzzy Sets Syst. **248**, 138–155 (2014). doi:10.1016/j.fss.2013.11.006
49. Chen, M., Ge, S.S.: Adaptive neural output feedback control of uncertain nonlinear systems with unknown hysteresis using disturbance observer. IEEE Trans. Ind. Electron. **62**(12), 7706–7716 (2015). doi:10.1109/tie.2015.2455053
50. Chen, M., Yu, J.: Adaptive dynamic surface control of NSVs with input saturation using a disturbance observer. Chin. J. Aeron. **28**(3), 853–864 (2015). doi:10.1016/j.cja.2015.04.020